# Accepted Manuscript

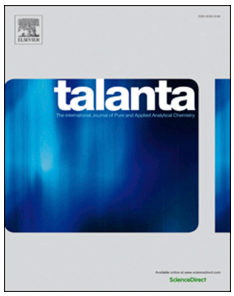


Artesunate-luminol chemiluminescence system for the detection of hemin

Tadesse Haile Fereja, Shimeles Addisu Kitte, Wenyue Gao, Fan Yuan, Dmytro Snizhko, Liming Qi, Anaclet Nsabimana, Zhongyuan Liu, Guobao Xu

PII: S0039-9140(19)30626-5

DOI: https://doi.org/10.1016/j.talanta.2019.06.007

Reference: TAL 20007

To appear in: *Talanta*

Received Date: 11 March 2019

Revised Date: 21 May 2019

Accepted Date: 3 June 2019

Please cite this article as: T.H. Fereja, S.A. Kitte, W. Gao, F. Yuan, D. Snizhko, L. Qi, A. Nsabimana, Z. Liu, G. Xu, Artesunate-luminol chemiluminescence system for the detection of hemin, *Talanta* (2019), doi: https://doi.org/10.1016/j.talanta.2019.06.007.

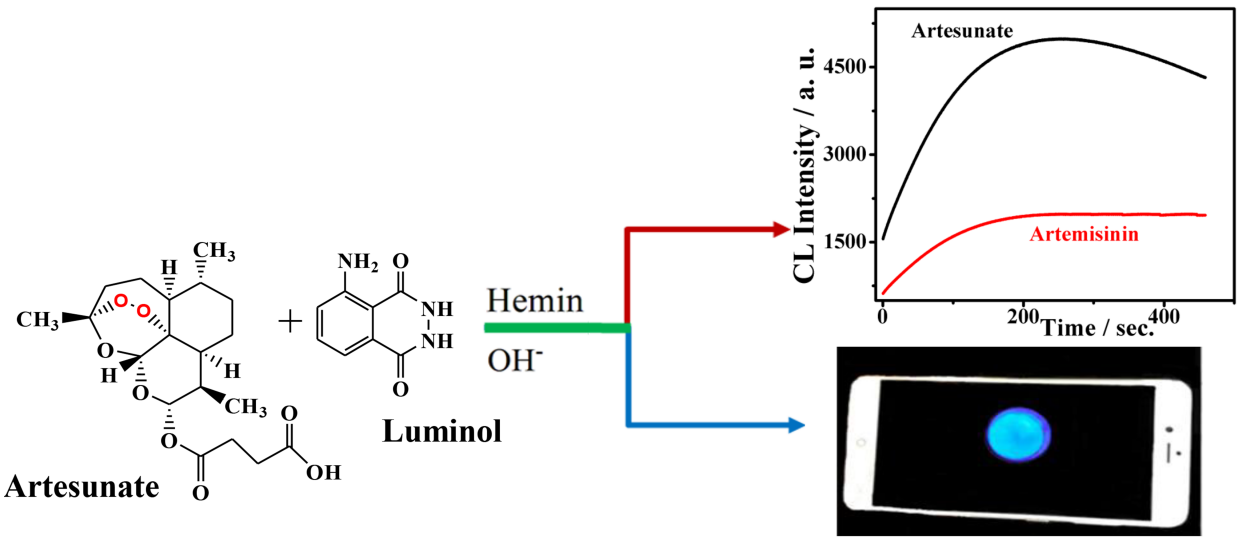

# Artesunate-luminol chemiluminescence system for the detection of hemin

Tadesse Haile Fereja,[a,b,c] Shimeles Addisu Kitte,[a,b] Wenyue Gao,[a,b] Fan Yuan,[a,d] Dmytro Snizhko,[a,e] Liming Qi,[a,b] Anaclet Nsabimana,[a,b] Zhongyuan Liu[a,*] and Guobao Xu[a,d*]

[a] State Key Laboratory of Electroanalytical Chemistry, Changchun Institute of Applied Chemistry, Chinese Academy of Sciences, 5625 Renmin Street, Changchun, Jilin 130022, P.R. China

[b] University of Chinese Academy of Sciences, Beijing 100049, P.R. China

[c] Ambo University, College of Medicine and Health Sciences, Department of Pharmacy, P.OBox 19, Ambo, Ethiopia

[d] University of Science and Technology of China. Anhui 230026, China

[e] Laboratory of Analytical Optochemotronics, Kharkiv National University of Radio Electronics, 14 Nauka Ave., Kharkiv 61166, Ukraine

## ABSTRACT

Fabricating simple, accurate and user-friendly diagnostic device for “point of care testing” (POCT) applications is one of the most challenging objectives in the analytical field. Hemin detection is important for drugs monitoring, diagnosis, and forensic latent bloodstain imaging. Herein is developed, luminol chemiluminescence biosensor for hemin detection using artesunate as coreactant. A possible mechanism to account for the chemiluminescence reaction is discussed. Hemin was detected using both photomultiplier tube (PMT) and smartphone as detector. The detection limit for hemin using smartphone as detector is 20 nM, enabling the visual detection of hemin in blood sample with a dilution factor of blood up to 120 000.While PMT detector is used, the system is able to detect hemin down to 0.22 nM. In addition to high sensitivity, this sensing system exhibit high selectivity. It can successfully distinguish bloodstain from other stains while

applying the system for point of care testing using smart phone as detector. Moreover, the system can detect artesunate with a linear range from 0.1 nM to 1.0 μM with a limit of detection of 0.078 nM.

**Key words**: Chemiluminescence, Smartphone, Point of care testing, Hemin, Artesunate.

## 1. Introduction

Artesunate and its derivatives are sesquiterpene lactones with a 1,2,4-trioxane core incorporating an endoperoxide linkage that is essential for activity [1]. The endoperoxide linkage is a trigger, activated by iron-induced reduction inside the malaria parasite, which releases a cascade of reactive intermediates-cytotoxic free radicals, one or more high-valent iron-oxo intermediates, and electrophilic alkylating agents that ultimately cause fatal damage to the parasites [2-5].

Hemin consists of an iron (III) ion held in a heterocyclic ring, known as a porphyrin. A porphyrin ring contains four pyrrole molecules cyclically linked together with the iron (III) ion bound in the center. The hemin as an electron transfer medium was based on the reversible redox reaction of Fe (III)/Fe(II) [6-8]. It may serve as intracellular messengers that modulate gene expression, the opening of ion channels, micro-RNA processing and other physiological processes [7]. In addition, it also has an important role in the regulation of hemoglobin synthesis, prevents cardiac and diaphragm mitochondrial dysfunction in sepsis [9], regulates the activity of cytoplasmic DNA polymerase from erythroid hyperplastic bone marrow cells and reticulocytes [10], suppress human immunodeficiency virus (HIV)-1 infection of human monocytes through heme oxygenase induction [11-14]. Moreover, in the field of pharmacy, hemin is used in natural

iron supplements for the treatment of iron deficiency anemia, as a raw material for the preparation of anticancer and semi-synthetic bilirubin medicines. Hemin can react with artesunate in solution to generate free reactive oxygen species (ROS). In plasmodia, these reactive species thought to damage the bacterial DNA, which is underlying reason of the bacteriostatic effects [9,13,15-18].

Although hemin is essential, free excess hemin can trigger several toxic effects such as permeabilization of cellular membranes and oxidation of proteins, lipids, and nucleic acids [7]. It's also reported that hemin oxidize Low Density Lipoprotein (LDL), which aggravate the risk of atherosclerosis and is extremely cytotoxic to cultured aortic endothelial cells [12, 19].

Several methods have been developed for hemin detection, including chemiluminescence (CL) aptasensor based on hemin aptamer modified magnetic graphene oxide polymers (MGO@H-Atp@Co-PP) [8], nanocomposite crafted by grafting hemin-binding-aptamer (HBA) onto carboxylated graphene (COO-GR) [20], capped carbon dot fluorescent sensors systems, namely, CDs/$\beta$-cd, CDs/LMH [21], and CDs/Suc, spectrophotometric assay [6]. However, all these methods require sophisticated instrumentation, sensor modification for sensitivity enhancement and skilled operators. Artemisinin/luminol chemiluminescence system is also reported for hemin detection [22]. But some limitations are associated with the system, such as insolubility of artemisinin in water, very high pH and narrow linear range. All these limitations motivate researchers to look for new coreactants that can be compatible with biological system, soluble in water and provide higher sensitivity and selectivity.

In the field of healthcare self-management, the pervasive usage of smartphone detectors provides a revolutionary opportunity for directly readout optical signals [23]. Another important benefit associated is that smartphones could perform tests outside clinical laboratories, especially

in low resource settings for critical and emergency medicine [24]. Several examples have been recently reported showing the actual feasibility of using smartphone-based platforms to detect biomarkers and analytes of clinical interest in bodily fluids including sweat, blood, and saliva [25].

Keeping the above facts in mind, the present work is involved the use of artesunate as an alternative coreactant because artesunate has favorable water-solubility and its activity is at least five times higher than that of artemisinin [2, 26, 27]. It has also antibacterial [28], anti-angiotensin [29], and anticancer [30] properties. In comparison with artemisinin/luminol chemiluminescence system, artesunate/luminol chemiluminescence system eliminate the need of organic solvent, requires much lower pH and has wider linearity range for hemin detection. It enables the sensitive detection of artesunate with a limit of detection of 0.09 nM.

## 2. Experimental sections

### 2.1. Chemicals and reagents

Artesunate and luminol (> 98.0%) were purchased from TCI (Shanghai, China). Hemin (99.9%) and thiourea (99.0%) were supplied by Sinopharm Chemical Reagent Co. Ltd. (Shanghai, China). Superoxide dismutase (SOD) was purchased from Beijing HWRK Chem. Co. Ltd. (China) and sodium azide ($NaN_3$) from Tianjin Fuchen Chemical Reagents Factory (China). $CaCl_2$, $Fe_2(SO_4)_3$, $FeSO_4$, $CoCl_2$, $MgSO_4$, $Pb(CH_3COO)_2$, $CuSO_4$, and $ZnCl_2$ were supplied by Beijing Chemical Reagent Company (Beijing, China). L-proline (Pro), L-arginine (Arg), and D-phenylalanine (Phen), were bought from Shanghai Yuanju Biotechnology Co. Ltd. (Shanghai, China). Creatinine, cysteine, glutathione, uric acid, glucose, fructose and sucrose were purchased

from Sinopharm Chemical Reagent Co. Ltd. (Beijing, China). Ethylenediaminetetraacetic acid disodium salt (EDTA) was bought from Shanghai Sangon Company (Shanghai, China). Human whole blood sample was obtained from healthy volunteers from hospital. Stock solutions of hemin and luminol were prepared by dissolving certain amounts of luminol or hemin in 0.1 M NaOH solution. Artesunate was dissolved in 0.01 M $NaCO_3$. Chemiluminescence intensities were captured by a BPCL ultraweak luminescence analyzer supplied by the Institute of Biophysics, Chinese Academic of Sciences. The photomultiplier tube (PMT) voltage was kept at 600 V. The homemade CL cell was constructed by cutting one well from a standard polystyrene 24-well plates. The cell has an inner diameter of 1.6 cm. It was used to mix the solutions, for CL intensity and smartphone detection experiments.

2.2. Chemiluminescent hemin detection

The procedure for hemin detection was carried out by mixing 100.0 μM luminol with 1.0 μM of artesunate in homemade chemiluminescence cell and the mixture was diluted to 400.0 μL with 5.0 mM NaOH and then 5.0μL of different concentrations of hemin were added rapidly into the solution, mixed, and used for CL detection. Filter glasses with various band-passes at wavelengths of 400 nm, 425 nm, 440 nm, 460 nm, 490 nm, 535 nm, 555 nm, 575 nm, and 620 nm were used to measure the CL emission spectrum of this system.

2.3. Preparation of blood samples

Blood sample was prepared according to previous procedure [22] with slight modification. In short, 0.1 mL of blood collected from hospital and 5 mL of 0.1M PBS (pH = 7.4) were mixed with 1.0 mL 0.1M EDTA and centrifuged at 1500 rps for 30 min. The supernatants were

collected and diluted 20,000-fold times with PBS solution before detection.10.0 µL, 20.0 µL and 50.0 µL from diluted solution were poured onto homemade CL cell and then, 4.0 µL of 100.0 µM artesunate solutions and 80.0 µL of 0.5 mM luminol solution were mixed to the blood sample. The mixture solution was diluted to 400.0 µL with 5.0 mM NaOH.

2.4. Smartphone detection procedure

The smartphone detection for hemin was performed by mixing different concentration of hemin 20.0 µL with 10.0 µL 100.0 µM artesunate and80.0 µL 500.0 µM of luminol in 400.0 µL 5 mM NaOH solution. After 4 minutes, maximum CL emission observed, the solution put into a black box. To capture the CL images, Nubia Z17 min smart phone was used in its automatic mode and the exposure time was set to be 60 s. Image J 1.46 r (http://imagej.nih.gov/ij/docs/guide) software have been used to interpret the images to quantify the emitted light over the sample spot area and expressed as relative light units (RLUs).

## 3. Results and Discussion

3.1. The CL characteristics of the reaction system

Fig.1 A shows the CL profiles of luminol/hemin, luminol/artesunate, artesunate/hemin, and luminol/hemin/artesunate system. CL intensities of luminol/hemin, luminol/artesunate, and artesunate/hemin systems are weak.CL intensities of luminol/hemin/artesunate system is much stronger than that of luminol/hemin, luminol/artesunate, and artesunate/hemin systems, showing that hemin exhibited high catalytic activity for CL of luminol/artesunate system. The CL intensity of luminol/hemin/artesunate system reached a maximum value after 250 s, which indicated slow CL reaction and enables glowing for several minutes.

Fig.1Bshows the CL intensity–time curves of the hemin/luminol/$H_2O_2$ system (inset) and luminol/hemin/artesunate system. By comparison, the CL peak intensity of the luminol/hemin/artesunate system is 16 times higher than that of the hemin/luminol/$H_2O_2$ system. It indicates that artesunate is an efficient coreactant for hemin-luminol CL

Iron ions of hemin cause the generation of reactive oxygen species (ROS) from artesunate [2, 4, 17, 18, 31]. The reaction kinetics relays on the cleaving rate of the endoperoxide linkage of artesunate to generate effective reactive radicals as shown Scheme 1. Cleavage of the oxygen–oxygen bond during decomposition of hydrogen peroxide is catalyzed by hemin [26]. As observed from the CL kinetics of the system, it can be possibly concluded that the catalytic reduction of artesunate is similar to that of hydrogen peroxide. The effects on CL intensity after addition of varying concentrations of sodium azide-scavengers of singlet oxygen ($^1O_2$) [32], superoxide dismutase-scavengers of superoxide radical anion ($O_2^{\bullet-}$) [33], mannitol scavengers of ROS [17, 34, 35] and thiourea-scavengers of hydroxyl radical ($HO^{\bullet}$) [36] are studied to reveal the CL mechanism. As shown in Fig. S1 A & B, both sodium azide and thiourea have almost negligible effects while, superoxide dismutase and mannitol quench CL intensities, revealing that the generated radical is neither singlet oxygen ($^1O_2$) nor hydroxyl radical ($HO^{\bullet}$). The quenching effects observed from mannitol buttresses that there is a generation of ROS. These results showed that $O_2^{\bullet-}$ plays a vital role in the luminol/artesunate/hemin CL reaction. Maximum CL emission wavelength for mixture of luminol/hemin/artesunate is about 450 nm (Fig. S2) consistent with the typical spectrum of luminol [22, 37]. Therefore, the possible CL mechanism is proposed as shown in Scheme 1.

3.2. Optimization of CL reaction conditions

3.2.1. Effect of NaOH concentrations

It is well known that the luminol CL reaction often occurred in basic media, thus the effect of NaOH concentration on CL reaction was investigated. Different concentration solutions, i.e. 1.0 mM, 2.0 mM, 5.0 mM, 10.0 mM, 20.0 mM, 50.0 mM and100.0 mM NaOH were tested. Fig. S 3 A represents the CL intensity of different concentration of NaOH as a function of time and the CL intensity peak was dramatically increased with the increase of NaOH concentration. Fig. S3 B shows that the highest CL signal/noise was obtained in the 5.0 mM NaOH, above which the background (noise) signal of the system became higher. Therefore, 5.0 mM NaOH solution was selected for subsequent experiments.

3.2.2. Effect of the concentration of luminol

Luminol was the CL agent in the system. Hence, its concentration should be carefully optimized to ensure for maximum response, sensitivity and reproducibility. The effect of the concentration of luminol on the CL reaction was studied in the range of 0.1 μM–100.0 μM (Fig. S 3 C & D). It was found that the CL intensity was significantly increased with the increase of luminol concentration to 100.0 μM, above which the background signal was also enhanced, leading to the decrease of signal/noise ratio. The reason was that the number of luminol radical increased with increasing its concentration, which was beneficial to increase the CL intensity of the system. Thus, 100.0 μM luminol was selected for subsequent work.

3.2.3. Effect of artesunate concentrations and artesunate detection

The effect of artesunate concentration was also investigated in the range of 0.1 nM to 2.0 µM. As shown in Fig. 2 A, CL intensities increase with the increase of the concentrations of artesunate in the range of 0.1 nM to 2.0 µM, and when the concentration of artesunate was 1.0 µM CL intensity reached its maximum value. In order to obtain higher sensitivity and reproducibility1.0 µM was selected for the further experiment. The CL intensity curve has good linear relationship over log of artesunate concentrations from 0.1 nM to 1.0 µM (Fig. 2 B). The linear equation is CL = 1469 + 947log (artesunate conc.) with a correlation coefficient of 0.993. The limit of detection calculated according to USP 41 [38] (Appendix S1) was found to be 0.078 nM for artesunate (where n = 9, 95% CI, the standard error of regression line and the slope were obtained from the regression equation).

The linearity of the method was also validated using F-test and/or intercept to y-axis. According to various guidelines and articles on analytical method validation [39-41], it is important to measure the linearity of a calibration function by preparing a minimum of five concentration levels in triplicates. If the experimental data set describes a genuine linear calibration of the form given by Eq. $Y= \alpha X +\beta$, then the tabulated F-value ($F_{tabulated}$) must be greater than the calculated F-value ($F_{(I-2)/(IJ-I)}$). The calibration results of our method show that $F_{calculated}$ is less than $F_{tabulated}$ (Appendix S2A) with y-intercept of 1469 when 947log (artesunate conc.) is zero and $r^2$ = 0.993. Accordingly, there is a significant linearity in the reported data for determining artesunate using the proposed method.

A survey of the literature shows that this value (LOD) is better than the reported values for artesunate. By comparison, it is simple, rapid, and sensitive and has a cheaper than most of the previously reported artesunate detection methods (Table S 1).

3.3. Calibration curves and detection limits of hemin assay

The linearity and limits of detection (LOD) for hemin based on this new CL system was investigated. A linear relationship between the CL intensities and the concentration of hemin in a range from 0.8 nM to 1000.0 nM was observed as shown in Fig. 2C and D. The LOD for hemin was found to be as low as 0.22 nM (calculated using the same procedures as Section 3.2.3, where n = 12, 95% CI, the standard error of regression line and the slope were obtained from the regression equation). The regression equation was $I_{CL} = 342 + 8.2c$, where $I_{CL}$ is the chemiluminescence intensity and *c* is hemin concentration in nM. The linearity was also validated according to Section 3.2.3. Since $F_{calculated}$ is less than $F_{tabulated}$ (Appendix S 2 B), with y- intercept when no hemin concentration is found to be 324 and $r^2 = 0.993$; there is a significant linearity in the reported data for determining hemin using the proposed method. The relative standard deviation (RSD, n = 9) at the hemin concentrations of 100.0 nM, 400.0 nM and 600.0 nM were 1.8%, 2.6%, and 1.95 % respectively indicating an acceptable reproducibility for hemin detection. The LOD for this method is better than the reported values for hemin [6, 42]. By comparison Table 1, it is simple, cheap, rapid, sensitive and has a wider linear range than most of the previously reported methods. Taken together, the proposed method could be a potential platform for hemin detection.

### 3.4. Smartphone detection of hemin

Since PMT and CCD detectors are fragility and expensive, smart phone devices could offer adequate and alternative analytical performance to detect very weak light signals, such as those produced by bioluminescence reactions, with reasonable exposure time (e.g., few seconds, minutes). Fig. 3 I shows images collected with smartphone camera after mixing different concentration of hemin with 50.0 µM artesunate and 300.0 µM luminol. The camera was able to

image 0.02 µM of hemin. The results expressed as relative light units (RLU) [22, 24] were used to describe the relationship with the concentrations of hemin. A linear calibration curve in Fig. 3 II is obtained from 0.02 to 50.0 µM with a linear equation of CL (RLU) = 40.4 log (Hemin conc./µM) + 66.4($R^2$ = 0.991). The linearity was also validated according to Section 3.2.3. Since $F_{calculated}$ is less than $F_{tabulated}$ (Appendix S 2 C), $r^2$ = 0.991 and the y-intercept is found to be 66.4 there is a significant linearity in the reported data for determining hemin using the proposed method with smart phone camera. The detection limit is 0.02 µM.

3.5. Selectivity of the CL method for hemin detection

For a new analytical method, especially with potential applications in biomedical samples, selectivity study is important. Therefore, the effects of some metal ions and biomolecules to the CL intensities of the system was evaluated. Fig. S4A shows the CL intensities of amino acids, sugars, and urea mixed with artesunate/hemin/luminol system as blank. The results reveal that biomolecules have little effect on the CL intensities. The interference effect of typical metal ions, including $Mg^{2+}$,$Pb^{2+}$, $Ca^{2+}$, $Co^{2+}$,$Cu^{2+}$, $Fe^{3+}$, $Fe^{2+}$, $Zn^{2+}$ on this new CL method was also investigated. Fig. S4B shows that the increase in CL intensities is negligible with the addition of metal ions at higher concentrations (20.0µM). The above results indicating that this method has excellent selectivity.

3.6. Determination of hemin in the presence of the human blood serum

To demonstrate the potential application of luminol/artesunate system for determination of hemin in biological sample, the assay of hemin in human serum was performed. Specifically, a different concentration of hemin was mixed to 2000-fold diluted blood sample, and the results

obtained by the standard addition method were showed in Table S 2.The recovery of added hemin in the spiked blood samples ranged from 99.8% to 101.3%, and the relative standard deviations were no more than 1.8%. The above results suggested that the proposed approach is simple, sensitive, rapid and had potential bio-medical application.

In order to examine the smart phone detection limit for blood, the human blood samples were diluted with 0.1M PBS (pH = 7.4). The dilution factor (Df) was used as the unit to depict the performance of the tests [22, 45]. The CL imaging pictures of different dilution factors of blood and the corresponding calibration curve are shown in Fig.3III. The result shows the CL intensity has a good linear relationship with the logarithm of the dilution factor of blood (Fig.3IV). The linear relation is CL (RLU) = 334.75 – 68.7 log (Df), ($R^2$ = 0.991). The maximum dilution factor of blood detectable by a smart phone is 120, 000. A recovery study was also performed using smart phone camera, using the same procedure as above. In brief, three different concentrations of hemin (0.5 µM, 5 µM and 10 µM) were mixed to 2000-fold diluted blood sample, and the results obtained by the standard addition method were showed in Table S3.The recovery ranged from 97.8% to 101.3%, and the relative standard deviations were no more than 1.9 %. Table S4 shows the summary of the results for hemin detection using BPCL photomultiplier tube and smart phone camera detectors.

Forensic and diagnostic scientists are often asked to determine whether a particular stain is or is not blood during point-of-care-testing. To proof whether this method can differentiate blood stains from the most probable coexisting stains in diagnostic medical laboratories and forensic field, 2000-fold diluted human blood, water, coffee, urine, morning saliva and red tea were dripped onto different pieces of filter paper (Fig. 4I). The imaging reagents were added to the dried filter paper and used for CL imaging in a dark box. The results suggest that this method can

successfully distinguish bloodstain from other stains. In real life situation, it's common that blood stains are contaminated with other impurities such as saliva, coffee, urine, and etc. Fig. 4 II shows that this system also able to differentiate a blood stain contaminated with urine and saliva (Fig. 4II, a and a1), coffee and red tea (Fig. 4II, 4 b and b1), coffee and urine (Fig. 4II, c and c1) urine and red tea (Fig. 4II, d and d1)

## 4. Conclusions

In summary we demonstrated the use of smartphone camera to capture images and quantify the luminescence light produced by hemin/luminol/artesunate system. The finding of this study showed that our developed method was able to detect hemin in blood sample with a dilution factor up to 120,000. The developed method also showed excellent selectivity toward some interfering metal ions and biomolecules. It can differentiate blood stains from urine, morning saliva, coffee, water and red tea which are most probable coexisting stains in diagnostic medical laboratories and forensic field. In view of both favorable sensitivity and high selectivity, the present method is an appealing alternative. Compared with most of the literatures about hemin detection, the method we presented is cost-effective, convenient, and did not require any complicated synthetic procedures.

## Acknowledgement

This work was kindly supported by the National Natural Science Foundation of China [Nos. 21675148, 21874126, & 21505128], Ministry of Science and Technology of the People's Republic of China [No. 2016YFA0201300 and 2016CTF032], the Chinese Academy of Sciences

(CAS) - the Academy of Sciences for the Developing World (TWAS) President's Fellowship Programme, and the Chinese Academy of Sciences (CAS) President's International Fellowship Initiative (PIFI).

**Conflicts of interest**

There are no conflicts to declare.

**References**

[1] N. Klonis, D.J. Creek, L. Tilley, Iron and heme metabolism in Plasmodium falciparum and the mechanism of action of artemisinins, Current Opinion in Microbiology 16(6) (2013) 722-727.

[2] L. Tilley, S.A. Charman, J.L. Vennerstrom, Chapter 2 Semisynthetic Artemisinin and Synthetic Peroxide Antimalarials, Neglected Diseases and Drug Discovery, The Royal Society of Chemistry2012, pp. 33-64.

[3] J. Li, B. Zhou, Biological Actions of Artemisinin: Insights from Medicinal Chemistry Studies, Molecules 15(3) (2010) 1378-1397.

[4] M. Asano, H. Iwahashi, Determination of the structures of radicals formed in the reaction of antimalarial drug artemisinin with ferrous ions, European Journal of Medicinal Chemistry 127(Supplement C) (2017) 740-747.

[5] W.-M. Wu, Y. Wu, Y.-L. Wu, Z.-J. Yao, C.-M. Zhou, Y. Li, F. Shan, Unified Mechanistic Framework for the Fe(II)-Induced Cleavage of Qinghaosu and Derivatives/Analogues. The First

Spin-Trapping Evidence for the Previously Postulated Secondary C-4 Radical, Journal of the American Chemical Society 120(14) (1998) 3316-3325.

[6] M.E. Lombardo, L.S. Araujo, A.B. Ciccarelli, A. Batlle, A spectrophotometric method for estimating hemin in biological systems, Analytical Biochemistry 341(2) (2005) 199-203.

[7] K.S. Lee, L.D. Raymond, B. Schoen, G.J. Raymond, L. Kett, R.A. Moore, L.M. Johnson, L. Taubner, J.O. Speare, H.A. Onwubiko, G.S. Baron, W.S. Caughey, B. Caughey, Hemin Interactions and Alterations of the Subcellular Localization of Prion Protein, Journal of Biological Chemistry 282(50) (2007) 36525-36533.

[8] Y. Sun, Y. Wang, J. Li, C. Ding, Y. Lin, W. Sun, C. Luo, An ultrasensitive chemiluminescence aptasensor for indirect hemin detection based on aptamer recognition materials, New Journal of Chemistry 41(14) (2017) 6098-6104.

[9] G.S. Supinski, L.A. Callahan, Hemin prevents cardiac and diaphragm mitochondrial dysfunction in sepsis, Free Radical Biology and Medicine 40(1) (2006) 127-137.

[10] E. Lim, Joung, Y., Jung, S., Park, S.H., Park, J.H., Kim, S.Y. ... Yang, Y.M, Hemin inhibits cyclin D1 and IGF-1 expression via STAT5b under hypoxia in ERα-negative MDA-MB 231 breast cancer cells, International Journal of Oncology 36 (2010) 1243-1251.

[11] W.S. Sheng, S. Hu, A.R. Nettles, J.R. Lokensgard, G.M. Vercellotti, R.B. Rock, Hemin inhibits NO production by IL-1β-stimulated human astrocytes through induction of heme oxygenase-1 and reduction of p38 MAPK activation, Journal of Neuroinflammation 7(1) (2010) 51-55.

[12] S.J. Wilson, A.K. Keenan, Role of hemin in the modulation of $H_2O_2$-mediated endothelial cell injury, Vascular Pharmacology 40(2) (2003) 109-118.

[13] Y. Lin, M. Li, L. Huang, W. Shen, Y. Ren, Involvement of heme oxygenase-1 in β-cyclodextrin–hemin complex-induced cucumber adventitious rooting process, Plant Cell Reports 31(9) (2012) 1563-1572.

[14] N.G.A.A. Kappas, Pharmacological and Clinical Aspects of Heme Oxygenase, Pharmacological Reviews 60 (2008) 79-127.

[15] B. Panijpan, C. Mohan Rao, D. Balasubramanian, Interaction of antimalarial drugs with hemin, Bioscience Reports 3(12) (1983) 1113-1117.

[16] J.M. Combrinck, T.E. Mabotha, K.K. Ncokazi, M.A. Ambele, D. Taylor, P.J. Smith, H.C. Hoppe, T.J. Egan, Insights into the Role of Heme in the Mechanism of Action of Antimalarials, ACS Chemical Biology 8(1) (2013) 133-137.

[17] A.M. Gopalakrishnan, N. Kumar, Antimalarial Action of Artesunate Involves DNA Damage Mediated by Reactive Oxygen Species, Antimicrobial Agents and Chemotherapy 59(1) (2015) 317-325.

[18] N. Berdelle, T. Nikolova, S. Quiros, T. Efferth, B. Kaina, Artesunate Induces Oxidative DNA Damage, Sustained DNA Double-Strand Breaks, and the ATM/ATR Damage Response in Cancer Cells, Molecular Cancer Therapeutics 10(12) (2011) 2224-2233.

[19] H.S.J. G. Balla, J.W. Eaton, J.D. Belcher, and G.M. Vercellotti, Hemin: A Possible Physiological Mediator of Low Density Lipoprotein Oxidation and Endothelial Injury, Journal of the American Heart Association 11 (1991) 1700-1711.

[20] L. Gao, Y. Xiao, Y. Wang, X. Chen, B. Zhou, X. Yang, A carboxylated graphene and aptamer nanocomposite-based aptasensor for sensitive and specific detection of hemin, Talanta 132(Supplement C) (2015) 215-221.

[21] U. Baruah, N. Gogoi, G. Majumdar, D. Chowdhury, Capped Fluorescent Carbon Dots for Detection of Hemin: Role of Number of -OH Groups of Capping Agent in Fluorescence Quenching, ScientificWorldJournal 2013(2013) 529159.

[22] W. Gao, C. Wang, K. Muzyka, S.A. Kitte, J. Li, W. Zhang, G. Xu, Artemisinin-Luminol Chemiluminescence for Forensic Bloodstain Detection Using a Smart Phone as a Detector, Analytical Chemistry 89(11) (2017) 6160-6165.

[23] Q. Mei, H. Jing, Y. Li, W. Yisibashaer, J. Chen, B. Nan Li, Y. Zhang, Smartphone based visual and quantitative assays on upconversional paper sensor, Biosensors and Bioelectronics 75 (2016) 427-432.

[24] A. Roda, E. Michelini, L. Cevenini, D. Calabria, M.M. Calabretta, P. Simoni, Integrating Biochemiluminescence Detection on Smartphones: Mobile Chemistry Platform for Point-of-Need Analysis, Analytical Chemistry 86(15) (2014) 7299-7304.

[25] Z. Li, Z. Li, D. Zhao, F. Wen, J. Jiang, D. Xu, Smartphone-based visualized microarray detection for multiplexed harmful substances in milk, Biosensors and Bioelectronics 87 (2017) 874-880.

[26] Y. Chen, S.-M. Zhu, H.-Y. Chen, Y. Li, Artesunate interaction with hemin, Bioelectrochemistry and Bioenergetics 44(2) (1998) 295-300.

[27] R. Dai, X. Xiao, F. Peng, M. Li, G. Gong, Artesunate, an anti-malarial drug, has a potential to inhibit HCV replication, Virus Genes 52(1) (2016) 22-28.

[28] S. Appalasamy, K.Y. Lo, S.J. Ch'ng, K. Nornadia, A.S. Othman, L.-K. Chan, Antimicrobial Activity of Artemisinin and Precursor Derived from In Vitro Plantlets of Artemisia annua L, BioMed Research International Article 2014(2014) 215872.

[29] G. Oboh, F.O. Bello, A.O. Ademosun, A.J. Akinyemi, T.M. Adewuni, Antioxidant, hypolipidemic, and anti-angiotensin-1-converting enzyme properties of lemon (Citrus limon) and lime (Citrus aurantifolia) juices, Comparative Clinical Pathology 24(6) (2015) 1395-1406.

[30] J. Wang, J. Zhang, Y. Shi, C. Xu, C. Zhang, Y.K. Wong, Y.M. Lee, S. Krishna, Y. He, T.K. Lim, W. Sim, Z.-C. Hua, H.-M. Shen, Q. Lin, Mechanistic Investigation of the Specific Anticancer Property of Artemisinin and Its Combination with Aminolevulinic Acid for Enhanced Anticolorectal Cancer Activity, ACS Central Science 3(7) (2017) 743-750.

[31] N. Pandey, S. Pandey-Rai, Updates on artemisinin: an insight to mode of actions and strategies for enhanced global production, Protoplasma 253(1) (2016) 15-30.

[32] M. Bancirova, Sodium azide as a specific quencher of singlet oxygen during chemiluminescent detection by luminol and Cypridina luciferin analogues, Luminescence 26(6) (2011) 685-688.

[33] G.R. Buettner, C.F. Ng, M. Wang, V.G.J. Rodgers, F.Q. Schafer, A new paradigm: manganese superoxide dismutase influences the production of H2O2 in cells and thereby their biological state, Free Radic Biol Med 41(8) (2006) 1338-1350.

[34] T.P. Khaket, R. Ahmad, Biochemical Studies on Hemoglobin Modified with Reactive Oxygen Species (ROS), Applied Biochemistry and Biotechnology 164(8) (2011) 1422-1430.

[35] D.B. Jennings, M. Ehrenshaft, D.M. Pharr, J.D. Williamson, Roles for mannitol and mannitol dehydrogenase in active oxygen-mediated plant defense, Proceedings of the National Academy of Sciences 95(25) (1998) 15129-15133.

[36] B. Lipinski, Hydroxyl Radical and Its Scavengers in Health and Disease, Oxidative Medicine and Cellular Longevity 2011(2011) 809696.

[37] M. Saqib, S. Li, W. Gao, S. Majeed, L. Qi, Z. Liu, G. Xu, N-Hydroxysuccinimide as an effective chemiluminescence coreactant for highly selective and sensitive detection, Analytical and Bioanalytical Chemistry 408(30) (2016) 8851-8857.

[38] U.S.P. Convention, Statistical Tools for Procedure Validation General chapters : <1210> Volume 42(5) (2019) 515-524.

[39] ICHQ2B, Validation of analytical procedures, methodology.International Conference on the Harmonization of Technical Requirements for the Registration of Pharmaceuticals for Human Use, (ICH) Q2B (ICH) Q2B (1999) 1-7.

[40] P. Araujo, Key aspects of analytical method validation and linearity evaluation, Journal of Chromatography B 877(23) (2009) 2224-2234.

[41] S.V.C. de Souza, R.G. Junqueira, A procedure to assess linearity by ordinary least squares method, Analytica Chimica Acta 552(1) (2005) 25-35.

[42] B.H. Kang, N. Li, S.G. Liu, N.B. Li, H.Q. Luo, A Label-free, Highly Sensitive and Selective Detection of Hemin Based on the Competition between Hemin and Protoporphyrin IX Binding to G-Quadruplexes, Analytical Sciences 32(8) (2016) 887-892.

[43] Y. Shi, W.T. Huang, H.Q. Luo, N.B. Li, A label-free DNA reduced graphene oxide-based fluorescent sensor for highly sensitive and selective detection of hemin, Chemical Communications 47(16) (2011) 4676-4678.

[44] G. Guan, J. Sha, D. Zhu, Heparin-MPA dual modified CdS quantum dots used as a simple and rapid label-free fluorescent sensor for protamine and hemin detection, Microchemical Journal 133(Supplement C) (2017) 391-397.

[45] S.A. DeJong, Z. Lu, B.M. Cassidy, W.L. O'Brien, S.L. Morgan, M.L. Myrick, Detection Limits for Blood on Four Fabric Types Using Infrared Diffuse Reflection Spectroscopy in Mid- and Near-Infrared Spectral Windows, Analytical Chemistry 87(17) (2015) 8740-8747.

## Lengends

**Table 1.** Comparison of different analytical methods for hemin detection.

**Fig. 1**. (A) CL kinetic curves for reaction of artesunate/hemin, luminol/hemin, luminol/artesunate and hemin/luminol/artesunate (red) system. The inset shows the enlarged CL intensity−time curve for artesunate/hemin (black), luminol/hemin (blue), and luminol/artesunate (green). (B) CL kinetic curves for reaction of hemin/luminol/artesunate system (first four red color lines) and luminol/$H_2O_2$/hemin system (inset; four blue color lines). Final concentrations: 100.0 µM luminol, 1.0 µM artesunate, 0.4 µM hemin 1.0 µM $H_2O_2$, in 5.0 mM 400.0 µL of NaOH; Photomultiplier tube voltage: 600 V.

**Scheme 1**. The proposed reaction mechanisms for the artesunate/hemin/luminol CL system.

**Fig. 2.** (A) Chemiluminescence time curve for hemin/luminol system as function of different concentration of artesunate (B) a linear plot of CL intensity peak verse log(artesunate conc.). Inset; CL intensity peak curves for different concentration of artesunate from 0.0 nM to 2.0 µM. (C) Chemiluminescence emission spectra time curves of artesunate/luminol system in the presence of different concentration of hemin. (D) The CL peak intensity plotted as a function of the concentration of hemin. Inset: shows enlarged curves between concentration of hemin 0.8 - 20.0 nM and CL peak intensity. The concentration of hemin is 0.0, 0.8, 1.0, 5.0, 10.0, 20.0, 50.0, 100.0, 200.0, 400.0, 600.0, 800.0, 1000.0 nM; with 1.0 µM artesunate, 100.0 µM luminol.

**Fig. 3.** (I) The luminescent images of test samples upon additions of different concentration of hemin, which were taken by the smartphone detection setup. The concentrations of hemin from A to I are 0.02, 0.05, 0.1, 0.5, 1.0, 5.0, 10.0, 20.0 and 50.0 µM respectively. (II) Calibration curve of chemiluminescent intensities (RLU) of color images with the logarithm of hemin concentrations. (III) CL images acquired with the smartphone at increasing the dilution factors (from A to K are 400, 800, 1000, 1500, 2000, 5000, 10,000, 20,000. 50,000, 100,000 and 120,000 respectively times diluted) for human blood sample. (IV) Calibration curves for chemiluminescence intensities (RLU) of color images with the logarithm of dilution factors.

**Fig. 4. (I)** The day light images of filter paper after dipping with coffee (A), red tea (B), urine (C), morning saliva (D), blood (E), and water (F) stains. The corresponding CL images taken in a dark box after adding imaging reagents were shown from a - f. (II) The day light images of filter paper after dipping with urine and saliva(A) coffee and red tea (B), coffee and urine (C), urine and red tea (D); a – d are the corresponding images taken in a dark box after adding the blood stain and imaging reagents; a1 – d1 is also the corresponding images taken in a dark box after adding the imaging reagents without blood stain.

**Table 1.** Comparison of different analytical methods for hemin detection.

| Analytical method | Detection system | Linear range | LOD | Ref |
|---|---|---|---|---|
| Fluorescent | PPIX- G-quadruplexes[a] | 50-2250 nM | 36 nM | [42] |
| Chemiluminescence | MGO@H-Atp@Co-PP[b] | 800nM-480 $\mu$M | 3.9 fM | [8] |
| Squarewave voltammetry | COO-GR/HBA nano composite [c] | 1-150 nM | 0.64 nM | [20] |
| Fluorescent | CDs/$\beta$-cd, CDs/LMH, CDs/Suc[d] | 1 $\mu$M–23 $\mu$M | 1 $\mu$M | [21] |
| Fluorescent | AO–PS2.M/rGO[e] | 2.81-4.37 $\mu$M | 50 nM | [43] |
| Fluorescent | Hep-MPA-CdSQDs[f] | 0.167-42.45 $\mu$M | 48.6 nM | [44] |
| Spectrophotometry | Acidified chloroform extraction | 1.15 – 9.2 $\mu$M | 72 nM | [6] |
| Chemiluminescence | Artemisinin/luminolchemiluminescence | 1.0 - 100.0 nM | 0.37 nM | [22] |
| **Chemiluminescence** | Artesunate/luminolchemiluminescence | **0.8 –1000.0 nM** | **0.22 nM** | **This work** |

[a]PPIX-protoporphyrin IX , [b]Magnetic graphene oxide (MGO)-heminaptamer (H-Atp)-cobalt porphyrin (Co-PP), [c]Hemin– binding – aptamer(HBA)– carboxylatedgraphene(COO-GR),[d]Carbon dots (CDs) /$\beta$-Cyclodextrin ($\beta$-cd)- Lactose Monohydrate (LMH) – Sucrose (Suc), [e]G-quadruplex structure aptamer (PS2. M) – acridineorange (AO) - reduced graphene oxide (rGO), [f]Mercaptopropionic acid (MPA) and heparin (Hep) dual modified CdS quantum dots (Hep-MPA-CdS QDs).

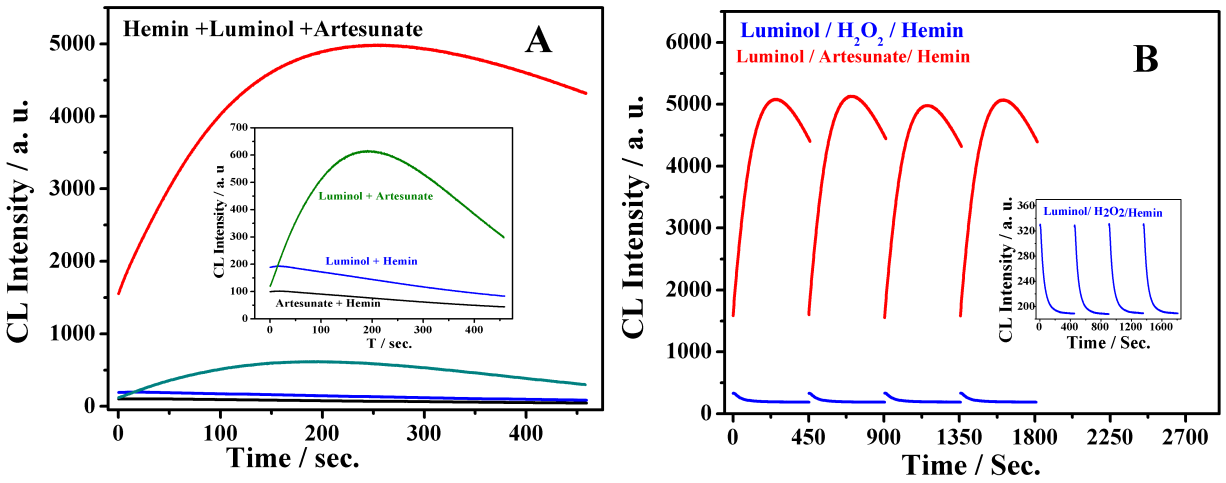

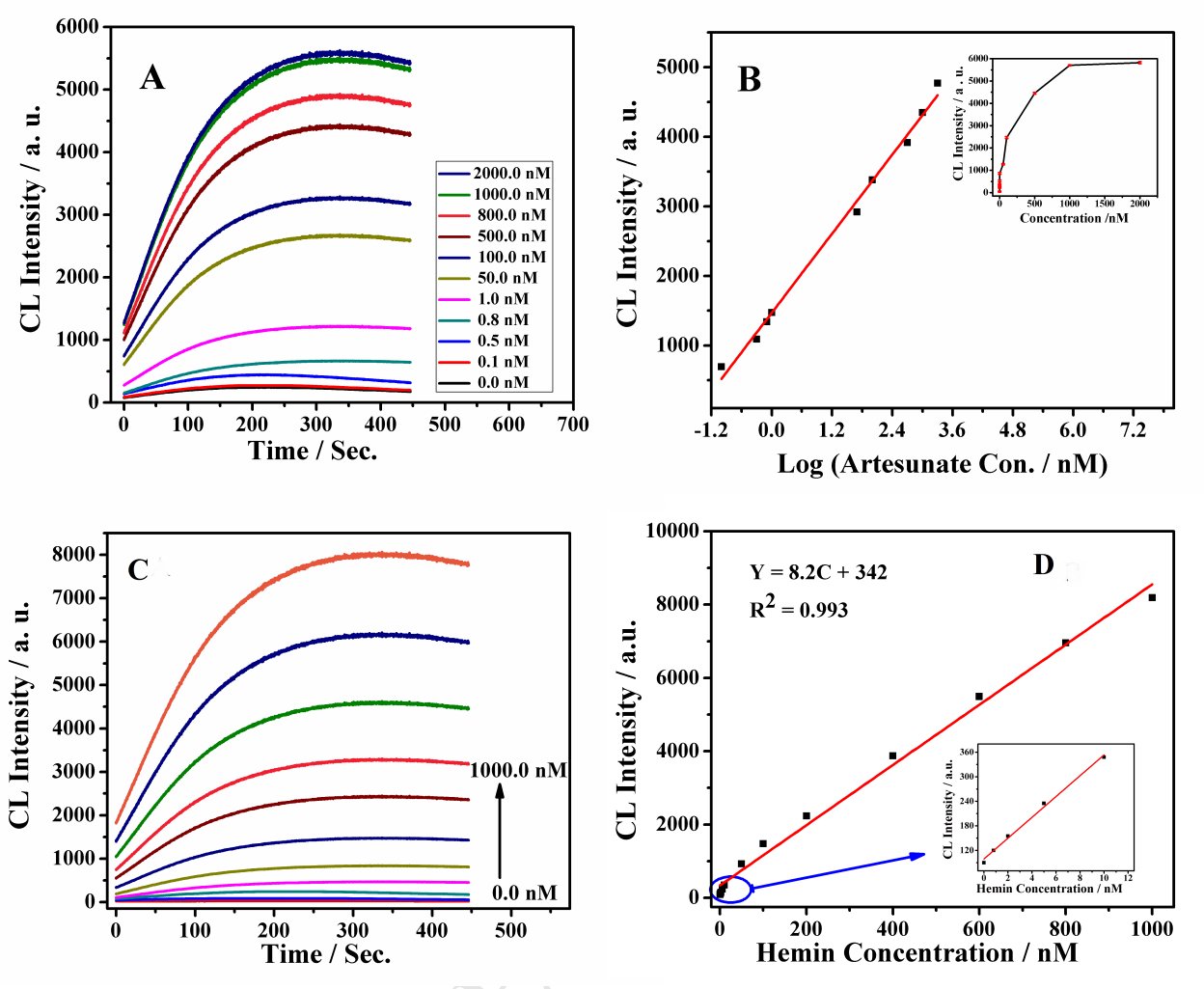
A
CL Intensity / a. u.
Time / Sec.
2000.0 nM
1000.0 nM
800.0 nM
500.0 nM
100.0 nM
50.0 nM
1.0 nM
0.8 nM
0.5 nM
0.1 nM
0.0 nM
B
CL Intensity / a. u.
Log (Artesunate Con. / nM)
CL Intensity / a . u.
Concentration /nM
C
CL Intensity / a. u.
Time / Sec.
1000.0 nM
0.0 nM
D
Y = 8.2C + 342
R2 = 0.993
CL Intensity / a.u.
Hemin Concentration / nM
CL Intensity / a.u.
Hemin Concentration / nM

I


III

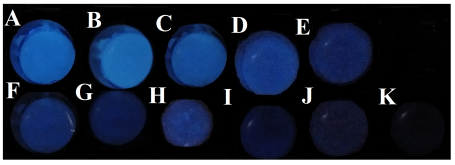


II

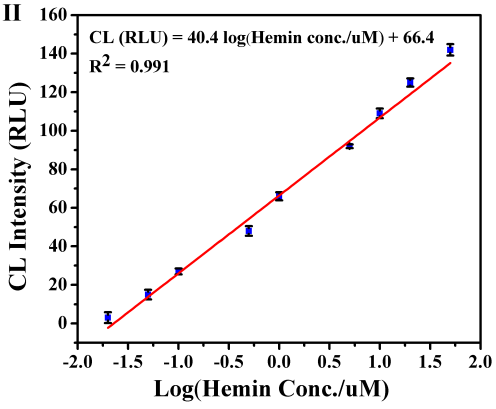


IV

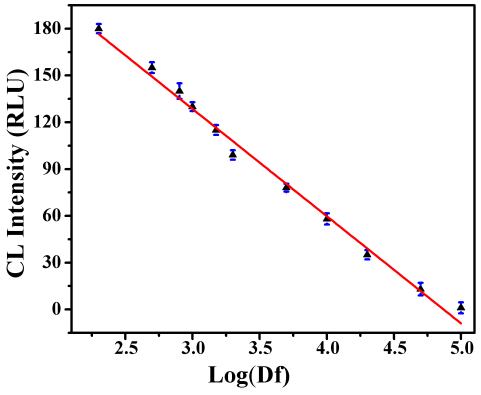

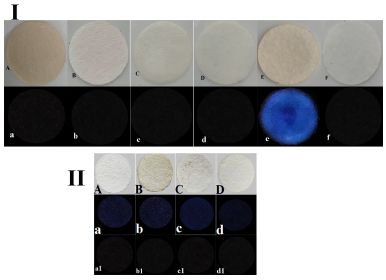

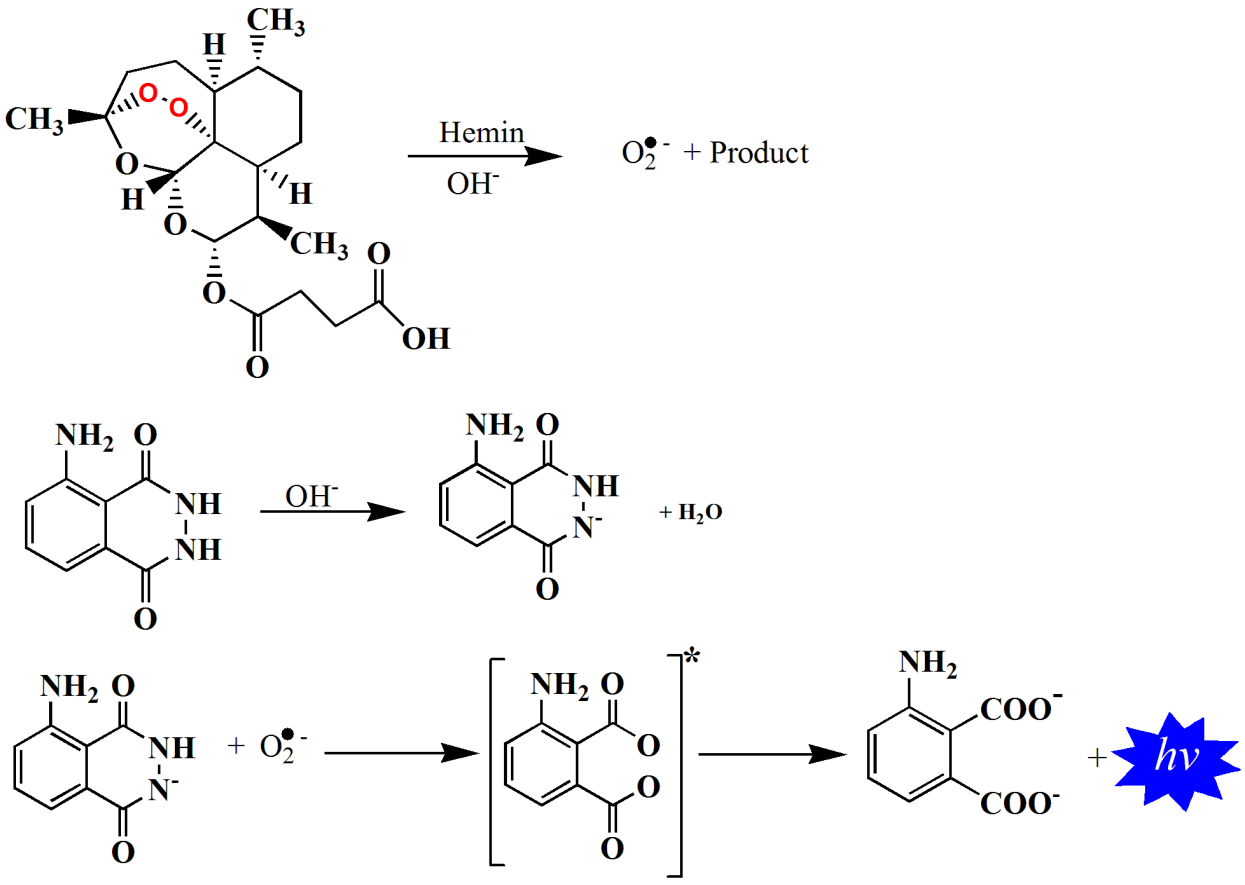

**Highlights:**

- The chemiluminescence of luminol-artesunate-hemin has been reported for the first time.
- Sensitive and selective detection of hemin using smartphone is achieved.
- The maximum dilution factor forlatent bloodstain imaging by a smart phone is 120, 000.
- The limit of detection for artesunate is 0.078 nM.